

Detection of stroboscopic effects in dependence of duty cycle, speed and illuminance level

Tianshu Chen, M.Sc., Dr.-Ing. Alexander Herzog, Prof. Dr.-Ing. habil. Tran Quoc Khanh;

Technische Universität Darmstadt, Laboratory of Adaptive Lighting Systems and Visual Processing, Hochschulstraße 4a, 64289 Darmstadt

chen@lichttechnik.tu-darmstadt.de

Abstract

Light-emitting diodes (LEDs) that are dimmed by pulse width modulation (PWM) may cause visually uncomfortable stroboscopic effects due to improper selection of operating parameters. Therefore, it is important to understand that the visibility of the stroboscopic effect depends on parameters such as duty cycle, speed, and illuminance level.

These dependencies were analysed by using a LED light source illuminating a black-coated rotating disk with a white dot mounted on top of it. Modulating the light source with a square wave signal between 100 Hz and 4200 Hz and different duty cycles (10%, 30%, 50%, 70%, 80%), allowed us to determine the subject's visibility of the stroboscopic effect for different rotation speeds (2m/s, 4m/s, 6m/s) and illuminance levels (100lx, 500lx, 1000lx).

Based on the results of these experiments, objective models were developed, which can be used to increase the accuracy and validity of the stroboscopic visibility measure, and effectively reduce the stroboscopic effects.

Index Terms: LEDs, PWM, stroboscopic effects



1 Introduction

Light-emitting diodes (LEDs) provide longer working lifespans and lower power efficiency compared with other types of lamps (e.g., incandescent, fluorescent, and high-intensity discharge lamps). LEDs offer several advantages, one of which is their ability to respond quickly to changes in the driving current. This attribute renders them highly suitable for pulse width modulation (PWM), enabling the rapid switching on and off of the digital signal to emulate diverse voltages. PWM is a widely adopted technique for dimming LEDs. In contrast to constant current dimming, the chromaticity shift caused by PWM dimming is visually unnoticeable.

However, LED lighting raises certain concerns one of which is called temporal artefacts (TLAs), such as flicker or the stroboscopic effect, resulting in unwanted visual discomfort in the presence of fast eye or object movements and possible negative health effects [1]. Firstly, there are the immediate results of a few seconds' exposure to TLAs, it can cause epileptic-sensitive photo spasms in various forms depending on the individual and its visual pathology, contrast, wavelength, and point of view or distance [2]. These symptoms are mostly associated with flickers in the frequency range between 3-100Hz [3]. Secondly, less obvious symptoms resulting from long-term exposure can occur, e.g., malaise, headaches, migraines, and impaired visual performance [4]. These symptoms are primarily associated with light modulations at higher frequencies (more than 100Hz) [5,6]. Most humans do not see Flicker exceeding 100Hz [7] but Berman et al. reported that flicker is transmitted through the retina up to 200Hz [8]. Flicker can occur because of 50Hz (in Europe, Asia, Africa, and Australia) or 60Hz (largely in the Americas) alternating current (AC) power line frequencies [9]. Therefore, to make the flicker imperceptible to the human visual system, high-frequency driving circuits such as electronic ballasts are used. Increasing the frequency of the driving circuit reduces the likelihood of visual artefacts being observed. However, high-frequency power supplies are generally more complex and expensive to produce, especially when low light levels are desired. In addition, high PWM frequencies may cause electromagnetic interference problems for surrounding electronic devices. Therefore, to reduce any potential negative health effects associated with LED lighting systems, it becomes crucial to gain a better understanding of the occurrence and visibility of temporal artefacts.

This paper begins by briefly reviewing the existing literature on the perception of Temporal Light Artefacts. Then, it introduces three perception experiments on the visibility of the stroboscopic effect. Based on the results of these experiments, objective models were developed, allowing us to predict the visibility of the stroboscopic effect for temporally modulated light sources under different situations.

2 Literature Overview

Flicker, stroboscopic effects and Phantom arrays are some of the well-known effects of Temporal Light Artefacts (TLAs). Flicker is a phenomenon that is defined as a visible

change in the brightness or color of a light source due to rapid fluctuations in the operating parameters. Flicker visibility has been studied extensively and it depends on many parameters (e.g., frequency and modulation depth) [10]. The acceptable level of flicker is defined by The Illuminating Engineering Society of North America, named Flicker Index (FI) [11]. It can vary between 0 and 1 and it is suggested to use systems that produce light with Flicker Index of 0.1 or less [11]. The Flicker Index is given by:

$$FI = \frac{A_1}{A_1 + A_2} \quad (1)$$

The area A_1 and the total area $A_1 + A_2$ are defined as shown in Figure 1. Another commonly used metric to evaluate flicker is the Flicker Percent [12,13]. It is also known as the modulation depth (MD) being defined as:

$$MD = \frac{L_{max} - L_{min}}{L_{max} + L_{min}} \quad (2)$$

L_{max} and L_{min} are the maximum and minimum luminance during one period. Both quantities are given by equations (1) and (2), respectively, and can be used to predict flicker visibility.

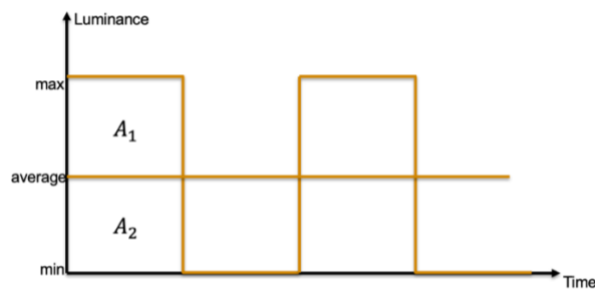


Figure 1. Illustration of the PWM dimming process

In contrast to flicker, the stroboscopic effect occurs with moving objects. The observer does not perceive a uniform motion of the object, but simultaneously several spatially delimited (discrete) images. Frier and Henderson [14] performed an experiment and observed that the visibility of the stroboscopic effect depends on the amplitude of the modulation in the light output. However, only qualitative observations, precise visibility measurements were not performed. Basically, there are different parameters that influence the cut-off frequency at which the effect is still perceptible. In 2011, Bullough et al. [5] concluded from their experiments with 50-120Hz that the perception of the effect depended not only on the frequency but also on the modulation depth and the duty cycle. Vogels et al. [15] studied its visibility threshold in terms of modulation depth using square waveforms with varying frequencies (50Hz, 100Hz, 200Hz, 400Hz). The visibility of the stroboscopic effect was confirmed to depend on the frequency and duty cycle of the square wave signal and on the speed of the rotating disk. Moreover, they indicated that the Flicker Index didn't account for the effect of frequency, so it was not a suitable measure for predicting the visibility of the stroboscopic effect, and a new measure should have been developed to predict it. Bullough et al. [9] examined the relationship between frequency (100Hz, 300Hz, 1000Hz, 3000Hz, 10000Hz) and

modulation depth and presented them in a joint function to gain a more understanding of the interaction of the two parameters. The authors concluded that both parameters interact with each other and thus created a basis for further research. However, the research only applied to a duty cycle of 50%. Perz et al. [3] performed an experiment with different frequencies (50Hz, 100Hz, 200Hz, 400Hz, 800Hz) and studied subjects' perceived visual artefacts even at frequencies of 800Hz depending on the modulation depth and waveform. Therefore, higher frequencies are required to eliminate stroboscopic effects. Zhao et al. [16] also investigated the short-term consequences of stroboscopic light for people under more intense conditions (100Hz, 400Hz, 1500Hz). The participants clearly perceived the discrete spatial movement and found the effect very unpleasant under the conditions presented. In addition, the participants also became increasingly tired.

To define a suitable metric for the Stroboscopic Effect, Perz and Wang et al. [3,17] conducted a study consisting of three experiments. These experiments formed the basis for the development of the Stroboscopic Effect Visibility Measure (SVM) and demonstrated the validity of this newly proposed metric. To further validate the SVM, Perz et al. conducted additional tests involving a larger number of subjects and frequencies and introduced the concept of a standard observer for precise SVM measurements. Perz et al. emphasized that the SVM was only valid for certain conditions in an office environment (illuminances around 500 lx and speeds of 4 m/s of the rotating disk). Therefore, Perz et al. called for further validation of the SVM in darker environments (e.g., street lighting) and for faster object movements (e.g., sports and industry for safety with fast rotating machinery) [18]. The Commission of the European Union also adopted the SVM metric and a limit of $SVM = 0.4$.

In typical interior-lighting applications, the most dominant visual artefact for frequencies higher than 100Hz is the stroboscopic effect and phantom array effect [19]. Hence, the goal of the study presented in this paper is to develop objective models, that allow us to predict the visibility of the stroboscopic effect for temporally modulated light sources under different constraints. This model can be used to effectively reduce the Stroboscopic effects and avoid possible health risks.

3 Experimental Methods

3.1 Apparatus

The experiments were performed on a rotating disk with a white spot mounted on top of it. The experimental setup is shown in Figure 2. A 25cm diameter disk with a black cotton surface and a white spot measuring 10mm in diameter was used. This setup provided a significant contrast between moving targets and backgrounds. The white spot was positioned 10.5cm from the center of the disk and rotated at different speeds (2m/s, 4m/s, 6m/s). It was considered appropriate for stroboscopic effects in office applications. The environment was completely darkened with black walls, and the tabletop was covered with a black cotton cloth. A chip-on-board LED (COB-LED) light

source with a color temperature of 4500K and a maximum power of 175W was used to illuminate a disk positioned on a table at different illuminance levels (100lx, 500lx, 1000lx). More information about the COB-LED used can be found in [20]. The height of the disk above the floor was 76cm, corresponding to the height of a regular desk. Luminance levels of the white spot were $15.5\text{cd}/\text{m}^2$, $75\text{cd}/\text{m}^2$, $158\text{cd}/\text{m}^2$, and the black backgrounds surrounding the white spot were $0.3\text{cd}/\text{m}^2$, $1.5\text{cd}/\text{m}^2$, $3\text{cd}/\text{m}^2$ and the remaining black areas had luminance levels of $0.00042\text{cd}/\text{m}^2$, $0.001\text{cd}/\text{m}^2$, $0.00198\text{cd}/\text{m}^2$, respectively. Distances from the subject to the center of the disk and between the subject's eyes and the stimulus were about 68cm and 66cm respectively, which was always kept constant by means of a chin rest. To drive the COB-LED, a dedicated LED driver was used, where both dimming methods (analog, PWM) can be used. It can supply a maximum current of 1A which is set by a relative voltage between 0 to 3.3V. The PWM signals were generated using Agilent's 33220A generator, which can set parameters such as frequency and duty cycle. The output signals were connected to the PWM inputs of the LED driver, using the Rohde & Schwarz NGE100 power supply series to supply 5V, from which the relative voltages of the LED driver and the rotating disk were also provided. Moreover, to control the function generator, a user interface was created in the programming language 'Python', where waveform (sine, square), amplitude, frequency, and duty cycle can be varied.

In conclusion, the basic parameters can be adjusted or changed by the experimental setup. Thus, it was possible to change speeds, stimulus shapes, and stimulus sizes. Furthermore, a square wave signal can be generated, in which amplitude, duty cycle, and frequency can be varied. Different illuminance levels can be set, varied, and kept constant in this experimental setup.

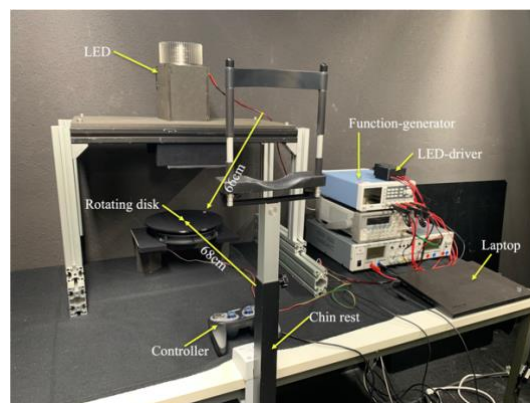
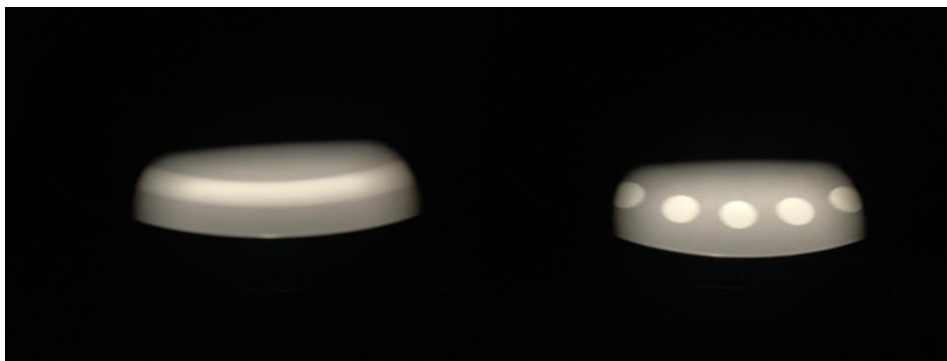


Figure 2. The experimental setup

3.2 Procedure

Participants were seated at 68cm from the center of the disk and the angle of view was approximately 7.8 degrees when the white dot passed the illuminated area. Next, they were given verbal instructions on the experimental procedure. Stroboscopic effects were thoroughly explained. They were also given a short demonstration of the test to familiarize them with the experimental procedure. Throughout the experiment, the disk

remained in constant rotation. Subsequently, the experiment started by switching on a DC light for 2s as the first step. Perz et al. [2] showed in the first measurement that a relative signal with a DC light before the actual stimulus was the most accurate method with the least variance. After 2s have elapsed, the modulated light was automatically switched on. Participants must indicate whether a difference between the DC light and the modulated light can be seen, and they were instructed to press the right key of the controller when they observed the stroboscopic effect on the rotating disk, and otherwise the left one. Lights were switched off for 1s after the input so that participants received the information that a new stimulus follows. The procedure started again from the beginning until all modulated stimuli had been presented. All responses of participants were stored in a CSV file. Combined with the method of constant stimuli, the 50 percent detection thresholds were derived for each condition tested. In addition, Figures 3(a) and (b) show close-up pictures of the rotating disk under two different lighting conditions: under DC illuminance, giving rise to the perception of a blurred image, and under AC modulated light, resulting in stroboscopic illuminance showing discrete movements of the spot.



Figures 3. (a) The rotating disk under DC illuminance and (b) the rotating disk under AC modulated light

In this experiment, the aim was to detect stroboscopic effects in dependence on duty cycle, speed, and illuminance. Before the data collection started, we did pre-experiments to determine the approximate range of the thresholds between 100Hz and 4200Hz. There were two steps in the experiment, where the first step was called low-resolution and the second was called high-resolution, in which 100Hz, 200Hz, 300Hz, 400Hz, 500Hz, 600Hz, 800Hz, 1000Hz, 1200Hz, 1400Hz, 1800Hz, 2200Hz, 2600Hz, 3000Hz, 3400Hz, 3800Hz, 4200Hz were tested in the first step to obtain estimated thresholds, in the second step, absolute thresholds were obtained by measuring 5 values from the left and right of estimated values, depending on the different resolutions. A light source with square wave signals and different duty cycles (10%, 30%, 50%, 70%, 80%) was used. The stimulus was repeated four times in random order under different rotation speeds (2m/s, 4m/s, 6m/s) and illuminance levels (100lx, 500lx, 1000lx). It usually took less than 30 minutes for every subject to observe each experiment situation. Five subjects (3 males and 2 females with ages ranging between 22 and 35) participated in the study to evaluate the detection and acceptability of stroboscopic effects. Since the stroboscopic effect was produced by flickering light

sources, we excluded participants that might be oversensitive to temporal modulations in light output. Such as, we only included participants that did not suffer from epilepsy nor had a family history of epilepsy, and that did not suffer from migraines.

4 Experimental Results

The objective of this experiment was to examine the relationship between stroboscopic visibility and the duty cycle. The data of four subjects (2 females and 2 males) was used to establish a model, while an additional male participant was used for evaluation purposes. The primary focus was to evaluate the responses of the four subjects to each duty cycle and frequency. The aim was to determine the threshold frequency, representing the frequency at which the detection probability reached 50 percent. For this purpose, logistic regression models were used. Figure 4 showed the logistic regression curves of one subject for different duty cycles under each case. A detection probability of 0% meant that the subject detected a stroboscopic effect four times at the respective duty cycle and frequency.

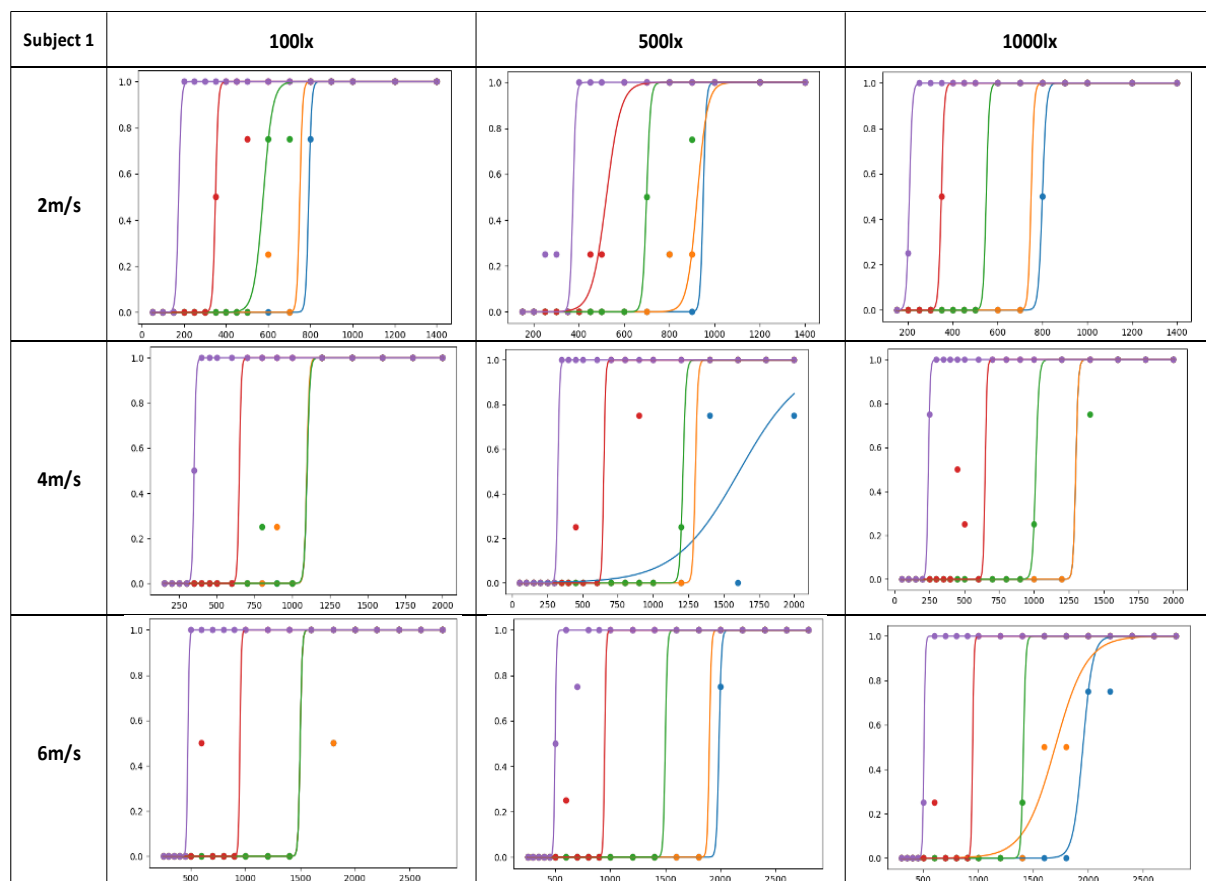


Figure 4. Logistic function of a subject for different duty cycles in each case

Basically, the threshold frequency decreased with increasing duty cycles for each subject. They showed similar behaviors that were the highest under 10% duty cycle and the lowest under 80% duty cycle. In the following, the frequencies were plotted as a function of the duty cycle at the visibility threshold as boxplots (Figure 5).

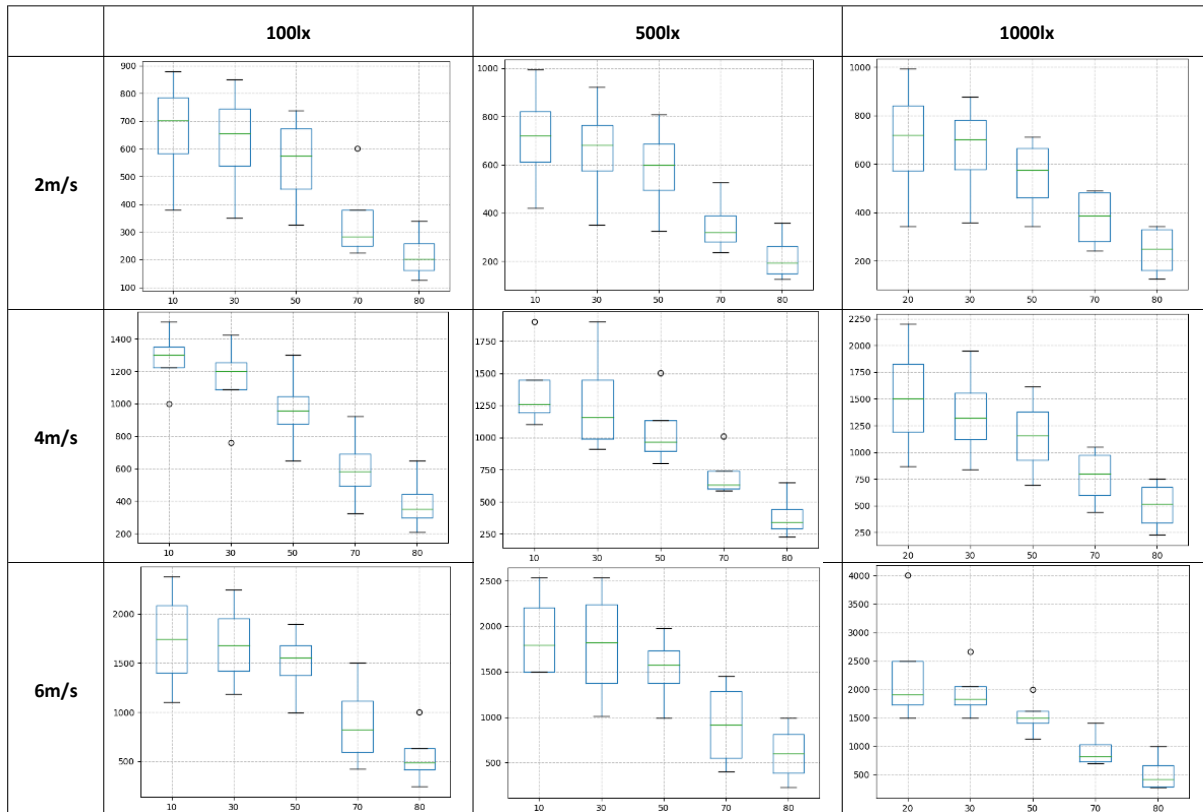


Figure 5. Boxplots of the absolute threshold frequency of all subjects for each case

Each figure presented a boxplot of the visibility absolute thresholds for each duty cycle that was tested in the experiment. The horizontal line in each box corresponded to the 50th percentile (i.e., the median). The lower and upper borders of the box corresponded to the 25th and 75th percentiles, respectively. The whiskers indicated the total range in measured thresholds, excluding outliers (which are defined as deviating more than 1.5 times half the width of the box). The one-factor analysis of variance (ANOVA) showed no significant difference between 10% and 50% duty cycle at a significance level of $\alpha = 0.05$.

The absolute thresholds varied widely due to each individual subjectivity, using these values directly for analysis can result in an overemphasis on data with higher numerical levels while underemphasizing those with lower levels. In order to enhance the reliability of the results, normalizing absolute thresholds proved to be a valuable step. The frequencies were represented by boxplots, illustrating their relationship between the duty cycle and the relative threshold defined at 10% duty cycle (Figure 6). The results illustrated a lower dispersion than the absolute thresholds at different duty cycles. Even though the variance of the conditions was different, an analysis of variance (ANOVA), a method used to test differences between two or more means resulting from parametric data, was performed to test for significant differences in the means of the conditions. There were no significant differences between the threshold frequencies at the 10% to 50% duty cycles after ANOVA at a significance level of $\alpha = 0.05$. A median difference of approximately 0.27 was determined. The differences were significant at the mean for duty cycles between 50% to 80%.

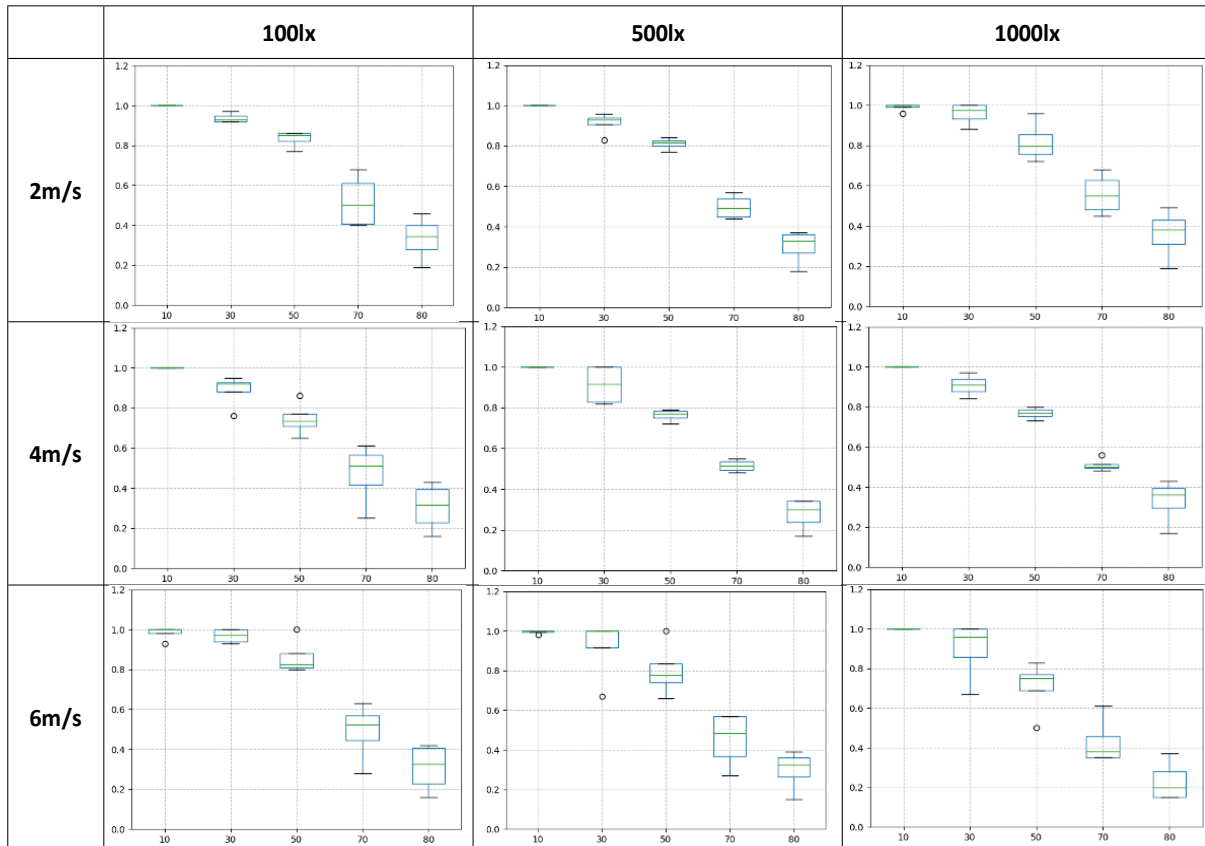


Figure 6. Boxplots of the relative threshold frequency of all subjects for each case

4.1 Effect of rotation speeds

This experiment investigated stroboscopic visibility in dependence of rotation speed. Figure 7 shows relative thresholds for participants at various duty cycles. The whiskers indicate the error bar with standard deviation. Also, the curves illustrate that behaviors of the threshold are relatively similar at different speeds (2m/s, 4m/s, 6m/s) respectively. Further, the results show a lower dispersion and smaller error for each case.

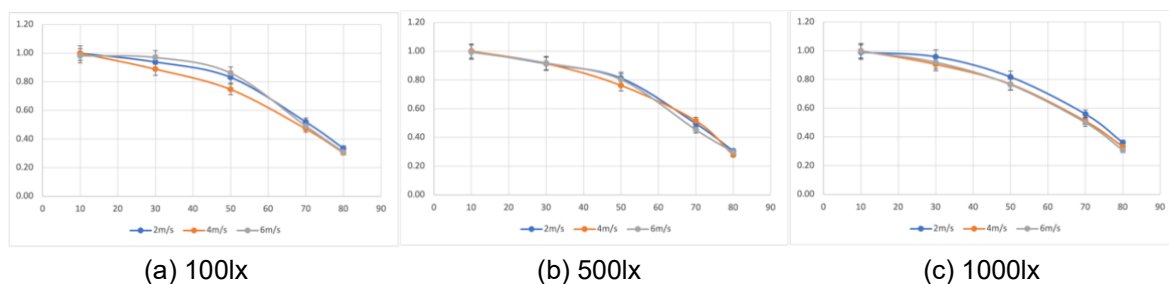


Figure 7. Relative threshold frequency depending on duty cycles and speeds at 100lx(a), 500lx(b), 1000lx(c)

Based on these data, Equation (3) can be used to model the dependence, where y is the relative threshold, x is the duty cycle and a, b are parameters. Figure 8 shows the relationship between relative thresholds and duty cycles under different illuminance levels, where Y-axis was relative threshold values and X-axis was duty cycles.

$$y = e^{ax^b} \tag{3}$$

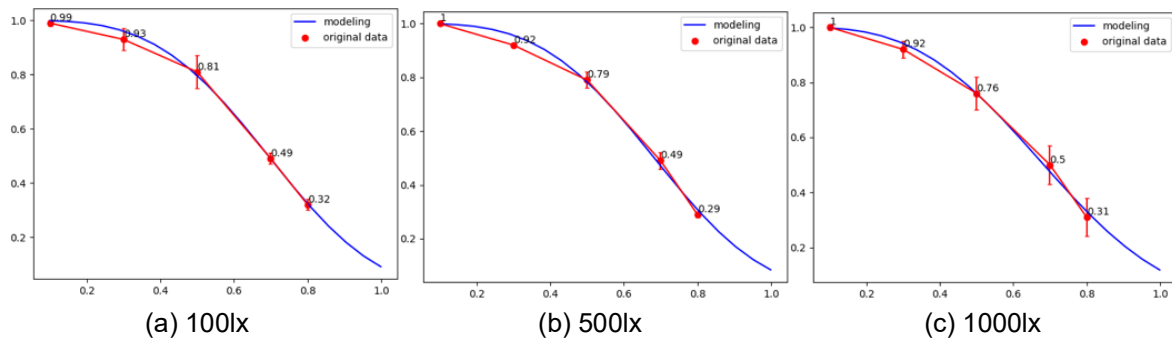


Figure 8. Modeling of stroboscopic effects in dependence of duty cycle with different speeds at 100lx(a), 500lx(b), 1000lx(c)

Figure 8 presents the fitting curves of the relative visibility threshold with its standard deviation (error bars). It is observed that the relative threshold of the stroboscopic effect decreases as the duty cycle increases. To quantitatively describe this relationship, Equation (3) is used, demonstrating excellent performance in the fitting. The optimal parameter values were determined by minimizing the sum of squared residuals, thus providing an accurate description of the relationship.

In order to further evaluate the accuracy and reliability of the model, additional analysis was conducted. Tables 1-3 in the Appendix list the absolute, predicted threshold frequencies and errors for the evaluator under different illuminance levels. Figure 9 shows the histogram of errors at 100lx, 500lx and 1000lx, in which the maximum is approximately 31%, but it is still in 95% confidence interval of absolute thresholds. In principle, minor deviations cannot be ruled out since subjects had different sensitivities. Overall, although there are small deviations from the predicted thresholds, the results at the different illuminance levels proved the validity and reliability of the model.

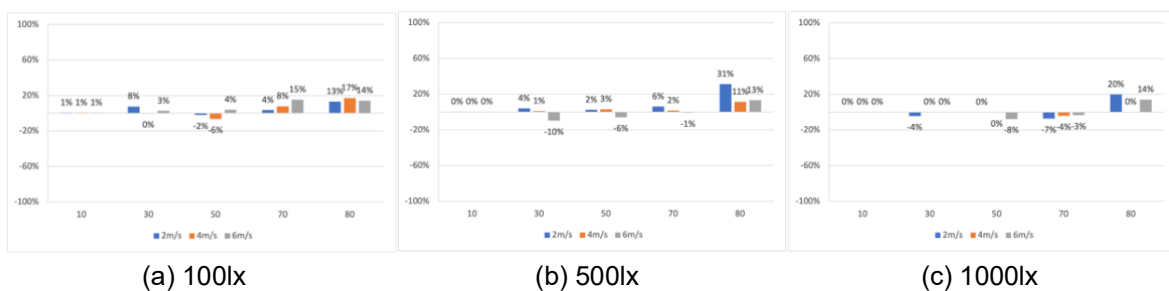
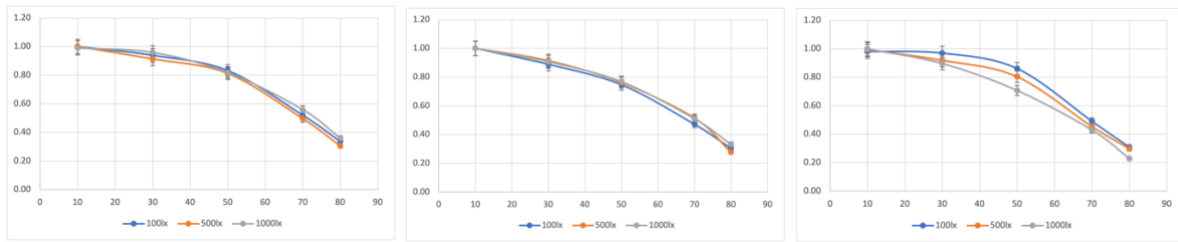


Figure 9. Modeling errors at 100lx(a), 500lx(b), 1000lx(c)

4.2 Effect of illuminance levels

This experiment aimed to investigate stroboscopic visibility in dependence of illuminance level. Figure 10 shows the relative threshold for participants at various duty cycles, in which the whiskers indicate error bars with standard deviation. Also, the behaviors of relative threshold curves are similar at different illuminance levels (100lx,

500lx, 1000lx). And the results show a lower dispersion and smaller error for each case.



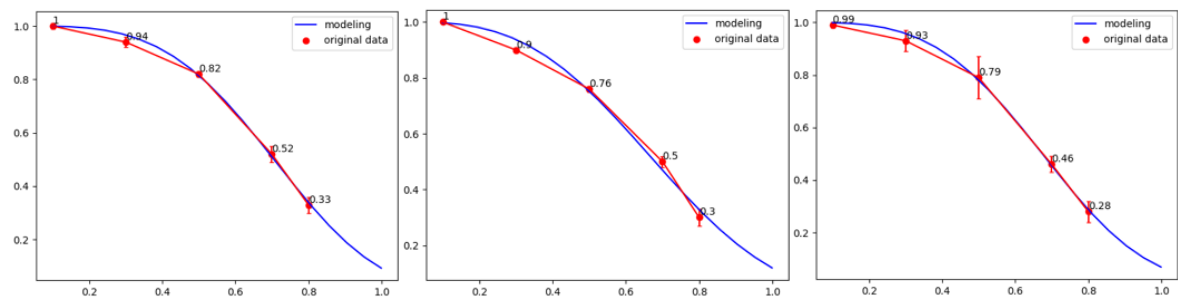
(a) 2m/s

(b) 4m/s

(c) 6m/s

Figure 10. Relative threshold frequency depending on duty cycles and illuminance levels at 2m/s(a), 4m/s(b), 6m/s (c)

In the following, functions can be modeled based on these data (Ref. Eq (3)). Equation (4) shows objective models. Figure 11 shows the relationship between relative thresholds and duty cycles under different speeds, where Y-axis was relative threshold values and X-axis was duty cycles.



(a) 2m/s

(b) 4m/s

(c) 6m/s

Figure 11. Modeling of the stroboscopic effect in dependence of duty cycle with different illuminance levels at 2m/s(a), 4m/s(b), 6m/s(c)

In Figure 11, the relative visibility threshold of the stroboscopic effect is shown, accompanied by error bars indicating the standard deviation. Notably, the threshold frequency of the stroboscopic effect exhibits a decreasing trend as the duty cycle increases. Equation (3) is used to quantify this relationship and exhibit excellent fitting performance. The determination of optimal parameter values is achieved by minimizing the sum of squared residuals, ensuring precise and accurate modeling of the relationship.

To assess the accuracy and reliability of the model, an additional analysis was carried out, aiming to provide a comprehensive evaluation of its performance. Tables 4-6 in Appendix show the absolute, predicted threshold frequencies and errors for the evaluator at different speeds. Figure 12 shows the histogram of errors at 2m/s, 4m/s and 6m/s, in which the maximum error value is approximately 25%, and still in 95% confidence interval of absolute thresholds. Therefore, these results provide evidence that the model is effective with different illuminance levels.

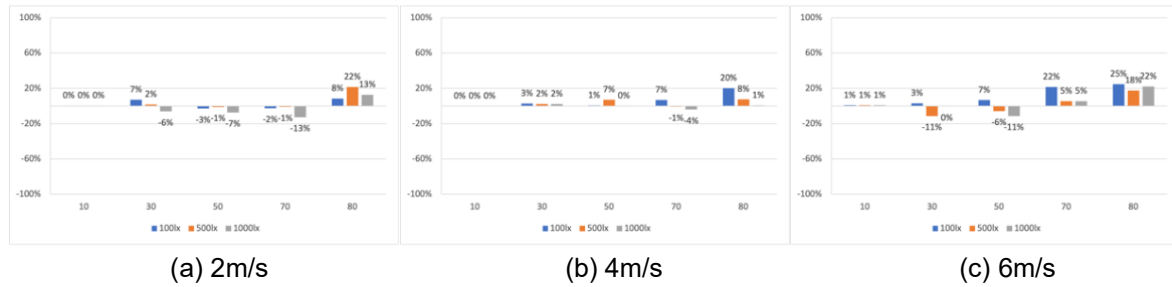


Figure 12. Modeling errors at 2m/s(a), 4m/s(b), 6m/s(c)

5 Discussion

The purpose of the experiments was to develop an objective model that effectively predicts the visibility of the stroboscopic effect. In the pre-experiment, we aimed to identify the specific range at which the threshold occurs by testing different frequencies. The results showed that the frequency range was between 100Hz to 4200Hz. Figure 5 showed the threshold of subjects can be up to 2000Hz and higher. Consequently, when comparing these findings with the SVM sensitivity curve, it became apparent that the application of the SVM is limited since it is only defined up to 2000Hz. We can also compare the absolute thresholds with the results previously reported. For instance, Bullough et al. [9] conducted their study using a white plastic rod measuring 172mm in length and 6mm in diameter, which was moved back and forth beneath the luminaire. In contrast, our study used a white spot with a diameter of 10mm, mounted on a rotating black surface. The observed threshold in Bullough et al.'s research was approximately 2400Hz under a 50% duty cycle, while in our study, it was approximately 1000Hz. Perz et al. [3,21] employed two luminaires that were mounted in a frame to illuminate the entire experimental section and placed next to a white wall. In our study, the environment was completely darkened with black walls. The COB-LED illuminated a specific portion of the rotation disk, leaving the rest in darkness. The observed threshold frequency under an illuminance level of 500lx was approximately 1250Hz in our study, while in Perz et al.'s research, it was 1110Hz. Furthermore, Perz et al. [21] used different illuminance levels, specifically 5lx, 10lx, 50lx, 100lx, and 500lx. Their ANOVA analysis confirmed that the highest threshold at 5lx was significantly different from the thresholds at all other illumination levels, and the lowest threshold at 50lx was significantly different from all other thresholds, except for the one at 100lx. In contrast, my study used illuminance levels of 100lx, 500lx, 1000lx as experimental parameters and the results indicated that the visibility of the stroboscopic effect has no significant difference between the illuminance levels of 100lx, 500lx, and 1000lx. The differences observed in the absolute thresholds between our study and previous research can primarily be attributed to differences in measurement methodology and various parameters used, such as speeds, duty cycles, and stimulus shape. Therefore, the variations in absolute thresholds should be primarily considered within the context of the variations in measurement techniques and experimental parameters employed across studies.

6 Conclusion

The current paper reports the detection of stroboscopic effects in dependence of duty cycle, speed, and illuminance. The study indicates that the threshold frequency has no significant differences between the 10% and 50% duty cycles. However, a noticeable decrease in threshold frequency is observed beyond 50% duty cycle. Additionally, the study involved the development of objective prediction models to determine the visibility of the stroboscopic effect. These models were specifically focused on speed and illuminance levels.

All experiments were performed with a maximum of five subjects. For a more accurate result, a higher number of subjects is necessary. Furthermore, the subjects are all healthy, so persons with low visual acuity suffering from (e.g., nystagmus) are not considered. This means that in the future investigations should also be carried out about the stroboscopic effect in particularly sensitive persons. Thus, health risks can be extended and possibilities to counteract the health consequences can be mentioned. In addition, other influencing parameters such as the stimulus shape, size, and luminance contrasts should be further investigated.

References

- [1] A. Wilkins, J. Veitch and B. Lehman, "LED lighting flicker and potential health concerns: IEEE standard PAR1789 update," 2010 IEEE Energy Conversion Congress and Exposition, Atlanta, GA, USA, pp. 171-178, 2010. doi: 10.1109/ECCE.2010.5618050.
- [2] F.H. Adler, R.A. Moses, and W.M. Hart, *Adler's Physiology of the Eye: Clinical Application*. 8th Edition. St. Louis: Mosby; 1987.
- [3] M. Perz, I. Vogels, D. Sekulovski, L. Wang, Y. Tu, and I. Heynderickx, "Modeling the visibility of the stroboscopic effect occurring in temporally modulated light systems," *Lighting Research & Technology*, pp. 281-300, 2015. doi:10.1177/1477153514534945
- [4] S.L. McColl, J.A. Veitch, "Full-spectrum fluorescent lighting: a review of its effects on physiology and health," *Psychol Med*, pp. 949-64, 2001 Aug. doi: 10.1017/s0033291701004251. PMID: 11513381.
- [5] J. Bullough, K. Sweater Hickcox, T. Klein, N. Narendran, "Effects of flicker characteristics from solid-state lighting on detection, acceptability and comfort," *Lighting Research & Technology*, pp. 337-348, 2011. doi:10.1177/1477153511401983
- [6] Rea, Mark, and M. Ouellette, "Table-tennis under High Intensity Discharge (HID) Lighting," *Journal of the Illuminating Engineering Society*, 1988. doi:10.1080/00994480.1988.10748705.
- [7] H. Apyrandi, P. Dupuis, N. I. Sinisuka and G. Zissis, "Stroboscopic Visibility Measure: assessment of pulsed light parameters," 2020 IEEE Industry Applications Society Annual Meeting, Detroit, MI, USA, pp. 1-4, 2020. doi: 10.1109/IAS44978.2020.9334755.
- [8] S.M. Berman, D.S. Greenhouse, I.L. Bailey, R.D. Clear, and T.W. Raasch, "Human electroretinogram responses to video displays, fluorescent lighting, and other high frequency sources," *Optom Vis Sci*. pp. 645-62, 1991 Aug. doi: 10.1097/00006324-199108000-00012. PMID: 1923343.
- [9] J. Bullough, K. Hickcox, T. Klein, A. Lok, and N. Narendran, "Detection and acceptability of stroboscopic effects from flicker," *Lighting Research and Technology*, pp. 477-483, 2012. doi:10.1177/1477153511414838.
- [10] H. de Lange DZN, "Eye's response at flicker fusion to square-wave modulation of a test field surrounded by a large steady field of equal mean luminance," *Journal of the Optical Society of America*, pp. 415–421, 1961.
- [11] Illuminating Engineering Society of North America, *IESNA Lighting Handbook*, 9th Edition, New York: IESNA, 2000.
- [12] A.J. Wilkins, *Visual Stress*, Oxford: Oxford University Press, 1995.

- [13] P.R. Boyce, *Human Factors in Lighting*, 2nd Edition, London: Taylor and Francis, 2003.
- [14] J.P. Frier, A.J. Henderson, “Stroboscopic Effect of High Intensity Discharge Lamps,” *Journal of the Illuminating Engineering Society*, pp. 83-86, 1973. doi: 10.1080/00994480.1973.10732230
- [15] I. Vogels, I. M., S. Sekulovski, and M. Perz, “Visible artefacts of LEDs,” In: *Proceedings of 27th Session of the CIE, Sun City, South Africa*, pp. 42–51, 2011.
- [16] X. Zhao, M. Li, Y. Lin, and W. Xu, “Study of the Stroboscopic Effect Visibility Measure (SVM) based on Cognitive Performance,” 2019 16th China International Forum on Solid State Lighting & 2019 International Forum on Wide Bandgap Semiconductors China (SSLChina: IFWS), Shenzhen, China, pp. 153-156, 2019. doi: 10.1109/SSLChinaIFWS49075.2019.9019756.
- [17] L. Wang, Y. Tu, L. Liu, M. Perz, I. Vogels, I. M., and I.E. Heynderickx, “50.2: Invited paper: stroboscopic effect of LED lighting,” *SID Symposium Digest of Technical Papers*, Bd. 46. 1. Wiley Online Library, pp. 754–757, 2015. doi: 10.1002/sdtp.10194.
- [18] M. Perz, D. Sekulovski, Vogels, I. M., and I.E. Heynderickx, “77-1: Invited Paper: Modelling Visibility of Temporal Light Artefacts,” *SID Symposium Digest of Technical Papers*, Bd. 49. 1. Wiley Online Library, pp. 1028–1031, 2018. doi: 10.1002/sdtp.12194
- [19] D. Polin, S. Klir, M. Wagner, and T. Khanh, “Reducing the stroboscopic effects of LED luminaires with pulse width modulation control,” *Lighting Research & Technology*, pp. 370-380, 2017. doi: 10.1177/1477153515615934
- [20] A. Herzog, M. Wagner, S. Benkner, B. Zandi, W. D. van Driel and T. Q. Khanh, “Long-Term Temperature-Dependent Degradation of 175 W Chip-on-Board LED Modules,” *IEEE Transactions on Electron Devices*, pp. 6830-6836, Dec. 2022. doi: 10.1109/TED.2022.3214169.
- [21] M. Perz, D. Sekulovski, I. Vogels, and I. Heynderickx, “Stroboscopic effect: contrast threshold function and dependence on illumination level,” *J. Opt. Soc. Am. A* 35, pp. 309-319, 2018. doi: 10.1364/JOSAA.35.000309.

Appendix

Table 1. The absolute, predicted threshold frequencies and error for one subject with different speeds at 100lx

DC	2m/s			4m/s			6m/s		
	Absolute (Hz)	Predicted (Hz)	Error (%)	Absolute (Hz)	Predicted (Hz)	Error (%)	Absolute (Hz)	Predicted (Hz)	Error (%)
10%	892	887	1	1700	1690	1	2573	2557	1
30%	900	832	8	1579	1585	0	2466	2399	3
50%	712	725	-2	1300	1382	-6	2180	2092	4
70%	457	441	4	911	840	8	1500	1271	15
80%	325	282	13	650	538	17	950	814	14

Table 2. The absolute, predicted threshold frequencies and error for one subject with different speeds at 500lx

DC	2m/s			4m/s			6m/s		
	Absolute (Hz)	Predicted (Hz)	Error (%)	Absolute (Hz)	Predicted (Hz)	Error (%)	Absolute (Hz)	Predicted (Hz)	Error (%)
10%	850	848	0	1838	1834	0	3100	3094	0
30%	810	778	4	1700	1682	1	2585	2837	-10
50%	690	673	2	1502	1456	3	2318	2456	-6
70%	442	415	6	911	897	2	1500	1513	-1
80%	362	249	31	607	539	11	1046	908	13

Table 3. The absolute, predicted threshold frequencies and error for one subject with different speeds at 1000lx

DC	2m/s			4m/s			6m/s		
	Absolute (Hz)	Predicted (Hz)	Error (%)	Absolute (Hz)	Predicted (Hz)	Error (%)	Absolute (Hz)	Predicted (Hz)	Error (%)
10%	850	847	0	1977	1971	0	3100	3090	0
30%	750	782	-4	1825	1820	0	2863	2854	0
50%	650	650	0	1504	1511	0	2201	2369	-8
70%	396	425	-7	950	988	-4	1500	1549	-3
80%	325	261	20	607	606	0	1107	951	14

Table 4. The absolute, predicted threshold frequencies and error for one subject with different illuminance levels at 2m/s

DC	100lx			500lx			1000lx		
	Absolute (Hz)	Predicted (Hz)	Error (%)	Absolute (Hz)	Predicted (Hz)	Error (%)	Absolute (Hz)	Predicted (Hz)	Error (%)
10%	892	889	0	850	847	0	850	847	0
30%	900	836	7	810	796	2	750	796	-6
50%	712	732	-3	690	698	-1	650	698	-7
70%	457	468	-2	442	446	-1	396	446	-13
80%	325	298	8	362	284	22	325	284	13

Table 5. The absolute, predicted threshold frequencies and error for one subject with different illuminance levels at 4m/s

DC	100lx			500lx			1000lx		
	Absolute (Hz)	Predicted (Hz)	Error (%)	Absolute (Hz)	Predicted (Hz)	Error (%)	Absolute (Hz)	Predicted (Hz)	Error (%)
10%	1700	1700	0	1838	1838	0	1977	1977	0
30%	1579	1535	3	1700	1659	2	1825	1785	2
50%	1300	1290	1	1502	1395	7	1504	1500	0
70%	911	849	7	911	917	-1	950	987	-4
80%	650	518	20	607	560	8	607	603	1

Table 6. The absolute, predicted threshold frequencies and error for one subject with different illuminance levels at 6m/s

DC	100lx			500lx			1000lx		
	Absolute (Hz)	Predicted (Hz)	Error (%)	Absolute (Hz)	Predicted (Hz)	Error (%)	Absolute (Hz)	Predicted (Hz)	Error (%)
10%	2573	2552	1	3100	3075	1	3100	3075	1
30%	2466	2388	3	2585	2877	-11	2863	2877	0
50%	2180	2034	7	2318	2450	-6	2201	2450	-11
70%	1500	1177	22	1500	1419	5	1500	1419	5
80%	950	715	25	1046	862	18	1107	862	22